EUROPEAN ORGANIZATION FOR NUCLEAR RESEARCH

L3 Note 2728
February 7, 2002

Search for Colour Singlet Exchange and Colour Reconnection Effects in Hadronic Z Decays from e^-e^+ Annihilation

The L3 Collaboration

Abstract

The structure of three jet events has been studied in hadronic Z decays to search for colour singlet exchange and colour reconnection effects in e^-e^+ annihilation. Particle flow and angular separation have been investigated in well separated symmetric 3 jet events from 75.1 pb^{-1} data collected by the L3 experiment. Asymmetries, defined in the inter-jet regions, are found to be sensitive to the exchange of a colour singlet instead of a colour octet gluon as well as effects of colour reconnection. From a comparison of the distributions between data and Monte Carlo predictions for colour octet and colour singlet production and also for colour reconnection models, limits are obtained on the fraction of of colour singlet exchange and on the colour reconnection probability.

1 Introduction

Bjorken [1] discussed the possibility of colour singlet exchange in hard diffractive hadron-hadron scattering characterised by large rapidity gap events. 1-2% of events with at least two high transverse energetic jets have been observed [2] to have no particle activity in large rapidity regions between the jets in $p\bar{p}$ collisions at Tevatron, Fermilab. 10% of all photo-produced di-jet events in deep-inelastic scattering at the HERA ep collider have also been reported to contain large rapidity gaps [3]. Using crossing symmetry arguments, gaps in three jet configurations can be expected to arise out of colour singlet exchange [4] in e^-e^+ annihilations as in $p\bar{p}$ collisions as depicted in the figure 1. A first investigation of rapidity gaps in e^-e^+ annihilations was performed by the SLD experiment [5]. In this analysis, a study of the gaps in symmetric three jet events from hadronic Z decays has been carried out.

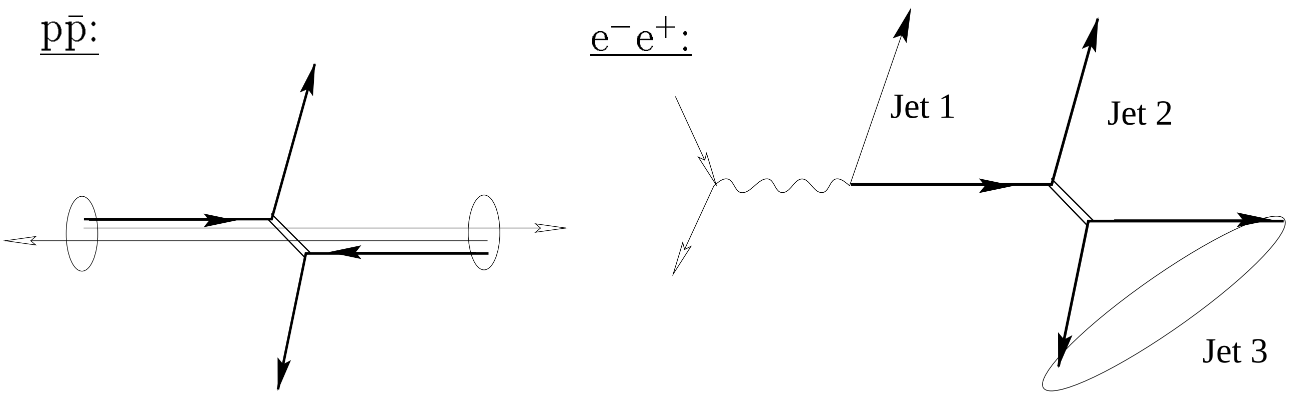

Figure 1: Colour singlet exchange in $p\bar{p}$ and in e^-e^+ reactions, depicted by double lines, as related by crossing symmetry.

When processes with large rapidity gaps occur in hadron-hadron or photon-hadron collisions it is possible that soft hadronic interactions between spectator partons produce particles that destroy the gap. The probability for this not to happen is called the 'gap survival probability'. A recent estimate [6] finds this probability to be $\simeq 20\%$ for $p\bar{p}$ collisions at $\sqrt{s} = 1.8$ TeV, appropriate for the DØ and CDF rapidity gap measurements. Thus the true rate of rapidity gap production in these events is estimated to be about $5 - 10\%$. The analysis based on data from e^-e^+ annihilation has the advantage that there are no 'underlying events' to dilute the fraction of rapidity gap events. However, the event statistics and maximum possible size of the rapidity gap are both smaller than in ep and $p\bar{p}$ collisions.

In the following, the data are compared to the predictions of pure colour octet (JETSET) and colour singlet exchange models. It should not be forgotten, however, that the fraction of colour singlet exchange processes expected on the basis of the ep and $p\bar{p}$ measurements is only $\simeq 10\%$.

Partons originated from a hard scattering process are eventually transformed into hadrons and this hadronisation process is usually described by non-perturbative models with specific assumption on the colour flow among the partons. In the simplest models the colour flow between two partons formed during the hard scattering phase has no interference from colour flow between other partons in the same process. However there may be interference effects in general which are termed as colour reconnection. This has a great relevance in the determination of W-mass from the effective mass of a two jet system coming from W-decays [7]. In three jet events, there is a colour flow between the quark and gluon. In presence of colour reconnection there will also be some effect seen between the quarks which will appear as a small admixture of colour singlet exchange. Such effects have been earlier investigated using charged particle multiplicity in gluon jets [8].

2 Methodology

2.1 Models

Specific models are chosen to describe colour octet exchange without colour reconnection effect, colour singlet exchange and colour octet exchange with colour reconnection effect.

The JETSET Parton Shower model [9] has been used to model colour octet exchange. The parameters of the model are tuned to match with the measured event shape distributions from the L3 experiment [10].

A toy model based on the colour flow of $q\bar{q}\gamma$ events is used to obtain the desired colour flow in colour singlet exchange [11]. Events of type $q\bar{q}\gamma$ with a photon effective mass as in the gluon jet mass distribution are generated, and the photon is then replaced by a boosted two jet event. This model (CS0) is illustrated in the figure 2. In another alternative model (CS2) studied, the photon is replaced by a gluon fragmenting independently. In terms of string fragmentation, coloured strings are thus confined to the $q\bar{q}$ gap, and lead to an increased hadronic activity in this gap and a reduction in the remaining ones.

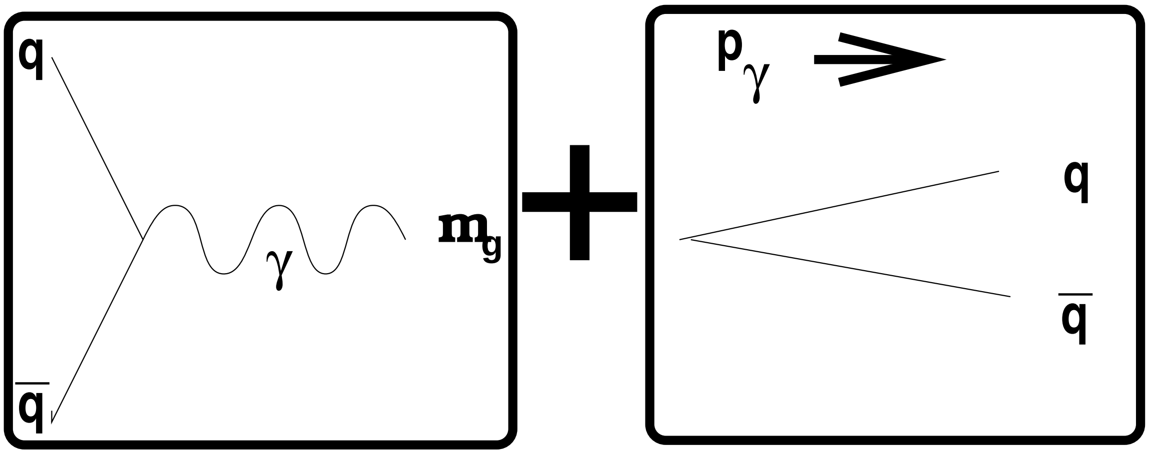

Figure 2: Model for colour singlet exchange.

A model based on generalised area law for hadronic string interactions due to Rathsman [12] is a QCD model including the colour reconnection effect. This model is tuned to describe the event shape data for three different values of the parameter R (0.0367, 0.1 and 0.2) which determines the probability of string re-interactions [13].

For comparison with data, events generated with JETSET, CS0 and CS2 models are passed through the L3 detector simulation [14] and reconstructed with the same algorithms used for analysing the data. The data, corrected from detector effects using the JETSET Monte Carlo sample on a bin-by-bin basis, are eventually used to compare with the different model predictions.

2.2 Variables

In order to look for colour singlet exchanges or colour reconnection effects, well separated completely symmetric three jet events are studied, and gaps between the jets are defined as regions outside the jet core. The events are clustered into jets using JADE [15] or $k_\perp$ [16] algorithms at fixed y_{cut}, and three jet configurations are retained. The angles (θ_{ij}) between the jets (i and j) projected onto the *event plane*, defined by the two most energetic jets, are restricted to lie within a 30° interval with respect to a perfect Mercedes 120° separation ($90^\circ < \theta_{ij} < 150^\circ$).

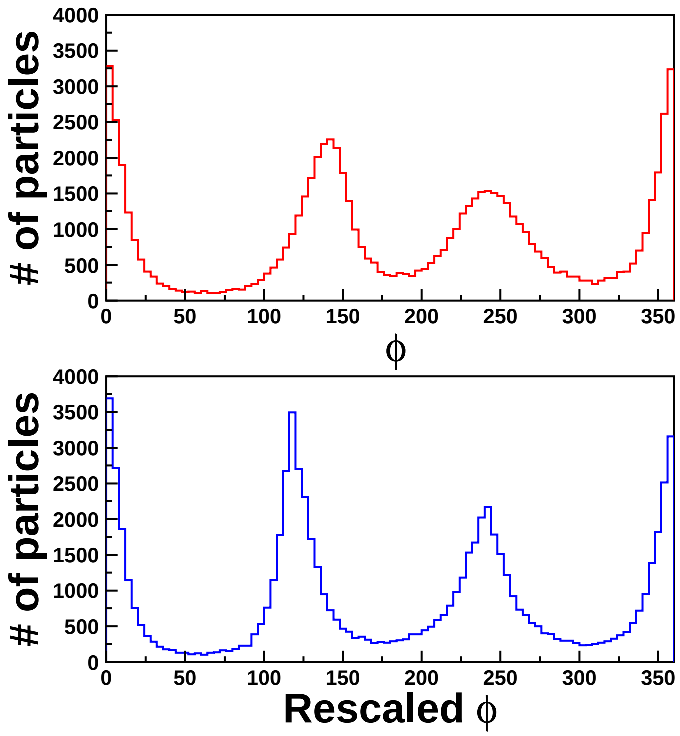

Figure 3: Flower plot for a sample of three jet events from JETSET Monte Carlo sample. The jets are reconstructed using JADE algorithm with $y_{cut} = 0.05$.

For uniformity in event-to-event comparison of angular distribution of particles, the angular separations between jets need to be standardised on an event-by-event basis. The angles projected on the event plane, ϕ, of all the particles in the event are rescaled such that the angle between the adjacent jets is strictly 120°. This gives the conventional flower plot as shown in the figure 3, with measured and rescaled angles for a sample of 3-jet events. Henceforth, in the discussion the angles are rescaled, and thus events can be superimposed to enable an event-by-event comparison of the angles between the particles.

The definitions of variables are motivated by the different particle multiplicity and angular separation in the gaps, as expected from differences in colour flow for colour singlet exchange (CSE) and colour octet exchange (COE): while in the latter there is colour flow between the qg and $\bar{q}$g and destructive interference between $q\bar{q}$, there is only colour flow between $q\bar{q}$ in the former case (see figure 4).

The jets are ordered in energy, so that the first two most energetic jets are most likely to be from the primary quarks. In order to minimise the bias from fragmentation, the core of the

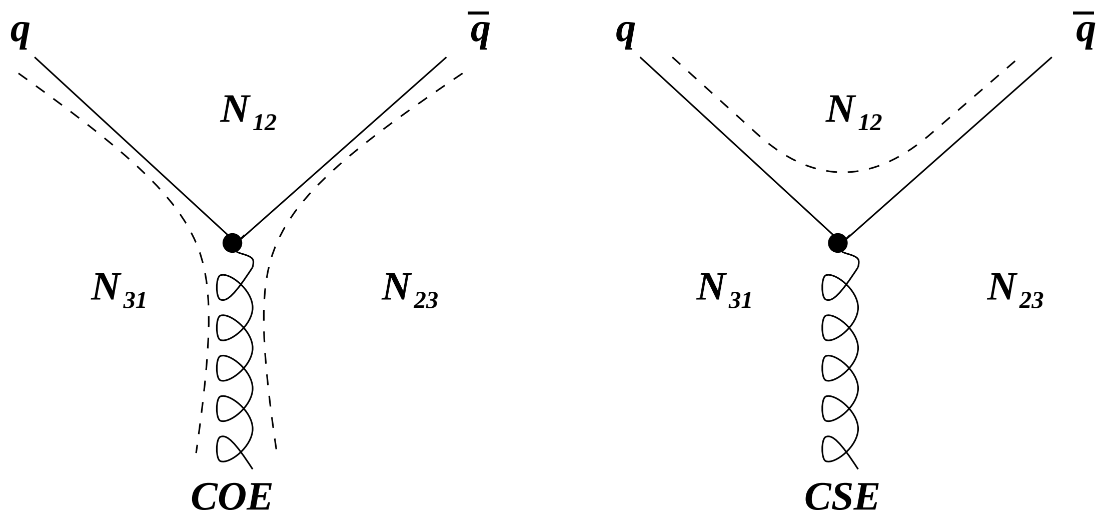

Figure 4: Comparison of colour flow in colour octet exchange (on the left) and colour singlet exchange (on the right).

jets is left out in the definition of the gaps. Accordingly, a cone is constructed around each of the 3 jets, with a fixed half angle $\mathrm{cone_{angle}}$. This study has been done for $\mathrm{cone_{angle}} = 15°, 20°$.

The colour exchange properties of the gaps can be studied using particle asymmetries. Let the number of particles in the the gap between jets i and j be N_{ij}. Then the particle asymmetry in the gap 12 is given by:

$$\mathrm{A}^{\mathrm{N}}_{12} = \frac{-\mathrm{N}_{12} + \mathrm{N}_{23} + \mathrm{N}_{31}}{\mathrm{N}_{12} + \mathrm{N}_{23} + \mathrm{N}_{31}} \, .$$

Similarly, one can define $\mathrm{A}^{\mathrm{N}}_{23}$ and $\mathrm{A}^{\mathrm{N}}_{31}$.

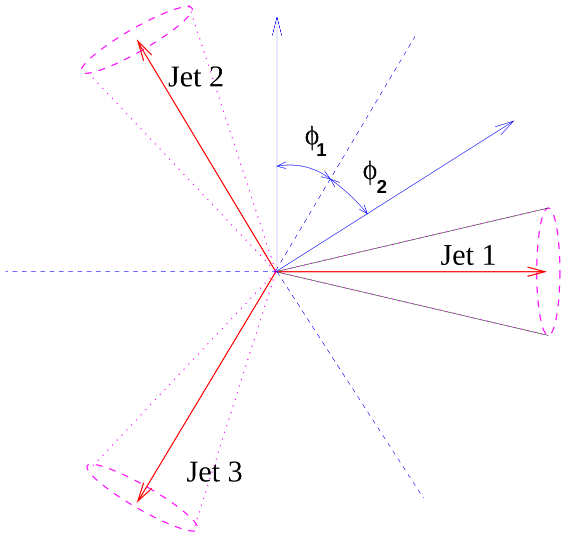

Figure 5: Angles in the gaps in Mercedes three jet events.

The properties of the gaps can also be studied in terms of the gap angles. Two definitions of angles are used: the minimum opening angle of the particles measured from the bisector in the gap (B-angle), and maximum separation angle between adjacent particles in the gap (S-angle). For example, the B-angle in gap 1 is: $B_{12} = \mathrm{Min}(\phi_1,\phi_2)$ (see figure 5). The angular asymmetry in gap 1 is defined as:

$$A^B_{12} = \frac{-B_{12} + B_{23} + B_{31}}{B_{12} + B_{23} + B_{31}} ;$$

similarly, A^B_{23} and A^B_{31} are defined. Alternatively, asymmetries can also be defined from the S-angle as:

$$A^S_{12} = \frac{-S_{12} + S_{23} + S_{31}}{S_{12} + S_{23} + S_{31}} ,$$

and similarly A^S_{23} and A^S_{31}.

The colour flow in the gaps between the quark and gluon jets is expected to give more particles and smaller angular separation than in the gap between the quark and colour singlet jets. Let us assume that the jets have been ordered such that the third jet is the gluon jet in the case of colour octet exchange. Typical ordering of variables as expected for the two scenarios are listed in the table 1 (ψ_{ij} stands for B-angle or S-angle in the gap ij), and illustrated in figure 4. Thus using these asymmetries one can distinguish between these two scenarios.

Colour Octet exchange	Colour Singlet Exchange
$N_{23} \approx N_{31} > N_{12}$ $A^N_{23} \approx A^N_{31} < A^N_{12}$	$N_{23} \approx N_{31} < N_{12}$ $A^N_{23} \approx A^N_{31} > A^N_{12}$
$\psi_{23} \approx \psi_{31} < \psi_{12}$ $A^\psi_{23} \approx A^\psi_{31} > A^\psi_{12}$	$\psi_{23} \approx \psi_{31} > \psi_{12}$ $A^\psi_{23} \approx A^\psi_{31} < A^\psi_{12}$

Table 1: Ordering of variables in singlet and octet exchange.

2.3 Sensitivity of Measurement

The average multiplicity for generated particles obtained from the colour singlet models are compared to that from the standard hadronic Monte Carlo generator JETSET [9] in the table 2. Also the number of particles in the $q\bar{q}$ gap, and the two other gaps averaged are compared for two definitions of the cone angle around the Mercedes jets. While the overall multiplicities are approximately the same in the colour octet and colour singlet models, the distribution of these particles in the inter-jet region are significantly different in the two cases.

	CS0	CS2	JETSET
Total	54.2 ± 0.1	54.8 ± 0.1	56.6 ± 0.1
$q\bar{q}$ GAP (15° cone)	7.25 ± 0.03	7.40 ± 0.03	5.46 ± 0.03
Other GAP (15° cone)	7.25 ± 0.03	7.20 ± 0.03	9.09 ± 0.02
$q\bar{q}$ GAP (20° cone)	5.70 ± 0.03	5.80 ± 0.03	4.12 ± 0.03
Other GAP (20° cone)	5.70 ± 0.03	5.80 ± 0.02	7.29 ± 0.02

Table 2: Average multiplicity for different models.

Figure 6 shows the particle flow distribution in the gap between the two quark jets and the corresponding asymmetry distribution for JETSET and two models with colour singlet exchanges. As can be seen from the plots, the asymmetry distribution is more sensitive to discriminate colour octet and colour singlet exchanges.

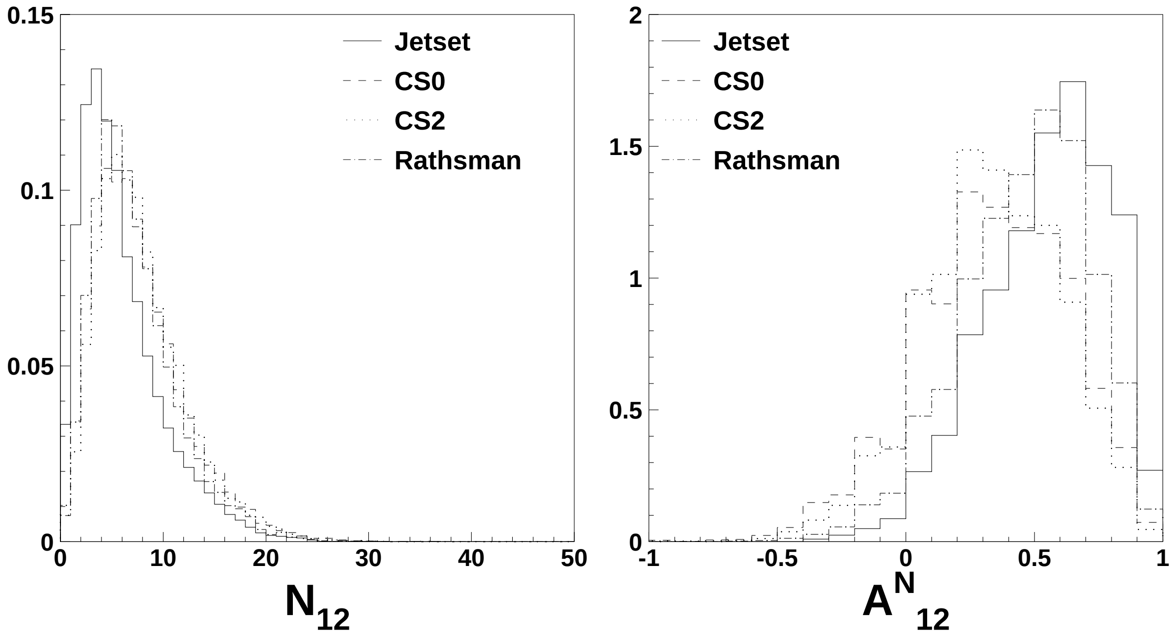

Figure 6: Particle flow in the gap between the two quark jets and the corresponding asymmetry for different models.

For energy ordered jets, the probability to have gluon in the least energetic jet is estimated to be 73% in 3-jet sample with $y_{cut} = 0.05$ (JADE algorithm), the probability reducing to 48% for Mercedes events. As a comparison, the asymmetry distribution of maximum separation angle in the gap between the two quark jets and two most energetic jets are shown in figure 7. It is clear that gluon enrichment in the third jet is crucial in improving the sensitivity of distinguishing colour singlet exchange from colour octet exchange.

3 L3 Data

The analysis is performed with data recorded by the L3 detector [17] during 1994-1995 data-taking periods at $\sqrt{s} \approx m_Z$. Two selections based on calorimetric clusters and charged tracks are applied. The criteria for event selection of Mercedes type three jet events are given in the table 3.

E^C, $E^C_{||}$ and $E^C_{\perp}$ are respectively the total energy observed in the calorimeters, the energy imbalance along the beam direction and the energy imbalance in the plane perpendicular to the beam direction. The cut on the number of calorimetric clusters, $N_{cluster}$, with energy greater than 100 MeV rejects low multiplicity events such as $\tau^-\tau^+$ final states.

N_{track} is the number of selected tracks. E^T, $E^T_{||}$, and $E^T_{\perp}$ are, respectively, the absolute momentum sum, the longitudinal and the transverse momentum imbalances computed from charged tracks. ϕ_2 is the second largest angle in the $R-\phi$ plane between two neighbouring tracks. This last requirement removes the remaining background due to $\tau^-\tau^+$ events where both the τ's decay through 3-prong final state. Each track is required to have a span of at least 30 $R-\phi$ hits (out of 62 wires), a distance of closest approach to the interaction point,

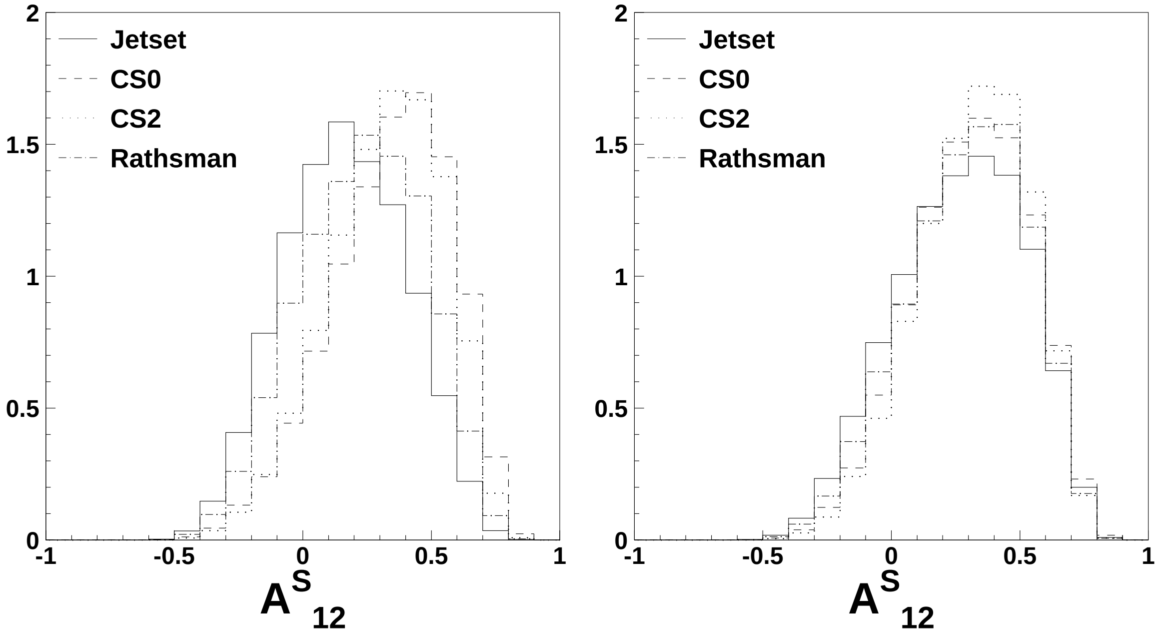

Figure 7: Distributions of the asymmetry in maximum separation angle between (a) the two quark jets and (b) between the two most energetic jets are compared for different models.

Calorimeter based	Charged-track based
$N_{cluster} > 12$	$N_{track} \geq 5$, $\phi_2 < 170^\circ$
$0.6 < E^C/\sqrt{\mathrm{s}} < 1.4$	$0.15 < E^T/\sqrt{\mathrm{s}}$
$\mid E^C_{\parallel} \mid /E^C < 0.40$	$\mid E^T_{\parallel} \mid /E^T < 0.75$
$E^C_{\perp}/E^C < 0.40$	$E^T_{\perp}/E^T < 0.75$
$N_{jets} = 3$	$N_{jets} = 3$
$\phi_{12}, \phi_{23}, \phi_{31} \quad \in \quad [90^\circ, 150^\circ]$	$\phi_{12}, \phi_{23}, \phi_{31} \quad \in \quad [90^\circ, 150^\circ]$

Table 3: Selection criteria for Mercedes type three jet events from hadronic Z decays.

in the plane perpendicular to the beam axis, of less than 20 mm and a measured transverse momentum with respect to the beam direction of greater than 100 MeV. The track polar angles are taken from matched calorimetric clusters.

L3 data from hadronic Z decays analysed correspond to a luminosity of 46.6 pb^{-1} from the 1994 and 28.6 pb^{-1} from the 1995 data taking periods. The number of hadronic events selected is 1949 K (1744 K) from cluster (track) based selection. The Monte Carlo event samples are reconstructed with the corresponding real detector conditions for each of the data taking periods. Fully simulated JETSET hadronic events are used as the colour octet Monte-Carlo, and simulations of three jet enriched samples of CS0 and CS2 events are used as colour singlet Monte-Carlos. In the following, the distributions from 1994 and 1995 data are added.

The events are clustered into jets using the JADE algorithm [15] with $y_{cut} = 0.05$ or the $k_\perp$ algorithm [16] with $y_{cut} = 0.01$ or 0.02. The gaps 23 and 31 are added and referred to as gap_{qg}. The fraction of three jet Mercedes type events are compared with data and Monte Carlo (JETSET) and listed in the table 4.

		JADE with $y_{cut} = 0.05$	$k_\perp$ with $y_{cut} = 0.02$	$k_\perp$ with $y_{cut} = 0.01$
DATA	Clusters	0.0357 ± 0.0001	0.0328 ± 0.0001	0.0281 ± 0.0001
	Tracks	0.0306 ± 0.0001	0.0255 ± 0.0001	0.0210 ± 0.0001
JETSET	Clusters	0.0378 ± 0.0001	0.0351 ± 0.0001	0.0307 ± 0.0001
	Tracks	0.0316 ± 0.0001	0.0270 ± 0.0001	0.0231 ± 0.0001

Table 4: Fraction of three jet Mercedes type events are compared for different jet algorithms, JADE and $k_\perp$.

3.1 Clusters in L3 Detector

To study the particle flow, two kinds of objects measured in the detector have been used, which show good matching of multiplicity between data and Monte Carlo:

- for the calorimeter based selection, calorimetric clusters with energy :
  - greater than 100 MeV in the electromagnetic calorimeter (ECAL) and > 900 MeV in the hadron calorimeter (HCAL), OR
  - greater then 100 MeV in ECAL with a minimum of 2 crystals hit, OR
  - greater then 1800 MeV in HCAL alone

  These cuts are used to avoid noisy clusters and take into account different thresholds in the different calorimeters;

- for the track based selection, charged tracks are required to have a minimum transverse momentum of 100 MeV, DCA (distance of closest approach) less than 20 mm, and hits of at least 20 wires in the central tracking chamber (TEC).

The mean values of the different types of cluster multiplicities are compared between data and Monte Carlo as given in the table 5. The distributions for track and cluster multiplicities are shown in the figure 8.

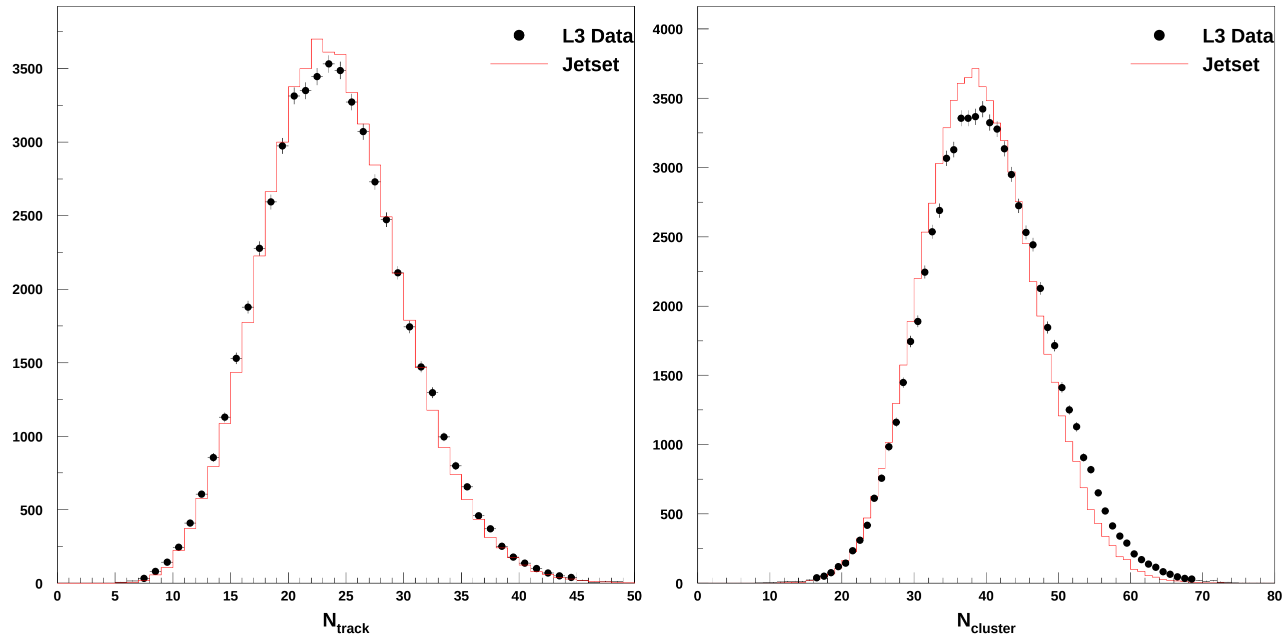

Figure 8: Distributions of charged particle multiplicity (left) and cluster multiplicity (right) for selected Mercedes events.

	Data	JETSET
$< N_{\mathrm{cluster}} >$	39.51 ± 0.03	38.53 ± 0.02
$< N_{\mathrm{track}} >$	23.41 ± 0.03	23.39 ± 0.01

Table 5: Mean cluster and track multiplicity for selected Mercedes events compared to Data and JETSET Monte Carlo.

3.2 Gluon Jet Identification

In order to maximise the sensitivity to differences in the gaps between $(q\bar{q})$ jets and gluon or colour singlet jets, gluon identification is necessary.

As one cannot use fragmentation properties to distinguish between quark jets and gluon/CS jets, jets tagged as b-jets are identified as quark jets.

The purity of the gluon in the third jet as seen in the detector worsens as compared to the generator level predictions when resolution effects are included. If one carries out detector reconstruction of Monte Carlo events from JETSET PS program according to the run condition of 1994-1995 data taking period, the probabilities of a gluon in the least energetic jet in three jet samples are 69 % and 59% when the jets are reconstructed from clusters and tracks respectively. For Mercedes criteria, these probabilities drop to 48% and 40% respectively, because of the symmetric configuration that dilutes the correlation between particle type and jet energy. The probability is smaller for jets made from tracks alone, because of smaller acceptance of the TEC.

We have used two approaches for tagging gluon jets: (1) a combination of energy ordering criteria and anti b-tagging of jets; (2) only anti b-tagging disregarding energy ordering criteria. The first method gives slightly better gluon purity but this reduces the number of selected events almost by a factor of 2 compared to the second method. Gluon tagging is done by demanding that two of the three jets should have b-tag discriminant [18] above a certain cut-off value ($B_{\rm jet}^{\rm mid}$) and the remaining jet should have the b-tag discriminant below a second cut-off value ($B_{\rm jet}^{\rm min}$). The purity of tagging for jets in Mercedes events and the number of selected events are given as a function of the cut values in the tables 6 and 7 for samples using clusters and tracks respectively (also see figure 9).

Selection			Jet algorithm used					
$B_{\rm jet}^{\rm mid}$	$B_{\rm jet}^{\rm min}$	Jet Order	JADE with $y_{\rm cut}=0.05$		$k_\perp$ with $y_{\rm cut}=0.02$		$k_\perp$ with $y_{\rm cut}=0.01$	
			Purity	# Events	Purity	# Events	Purity	# Events
0.00	10.00	Yes	0.480	69619	0.500	54805	0.488	63934
0.75	0.75	No	0.538	13724	0.545	10973	0.537	12747
0.50	0.75	Yes	0.598	9401	0.617	7515	0.608	8703
1.00	1.25	No	0.615	9455	0.625	7538	0.616	8769
0.75	1.25	Yes	0.662	6152	0.681	5017	0.665	5738
1.25	1.50	No	0.686	6258	0.695	5085	0.687	5871
1.00	1.25	Yes	0.721	3907	0.743	3219	0.726	3658
1.25	1.50	Yes	0.775	2668	0.792	2116	0.776	2516
1.75	1.25	No	0.808	2645	0.830	2180	0.816	2484
1.75	0.75	No	0.824	2189	0.841	1814	0.829	2055
2.00	1.25	No	0.856	1892	0.873	1574	0.859	1778
2.00	1.00	No	0.861	1762	0.879	1468	0.863	1663
2.00	1.00	Yes	0.896	826	0.920	721	0.900	799

Table 6: Number of selected gluon tagged events and gluon purity in the sample obtained using clusters are compared for different jet algorithms.

We have used $B_{\rm jet}^{\rm mid}=1.25$, $B_{\rm jet}^{\rm min}=1.50$ and jet energy ordering criteria to define the least energetic jet as the gluon jet in the Mercedes event sample using clusters. This cut corresponds to gluon purity of 77.5% in a sample of 2668 events. As a cross check we have used tracks to define Mercedes type events and use the cuts $B_{\rm jet}^{\rm mid}=1.75$, $B_{\rm jet}^{\rm min}=1.25$ to define the gluon jet as

Selection			Jet algorithm used					
B_{jet}^{mid}	B_{jet}^{min}	Jet Order	JADE with $y_{cut} = 0.05$		$k_\perp$ with $y_{cut} = 0.02$		$k_\perp$ with $y_{cut} = 0.01$	
			Purity	# Events	Purity	# Events	Purity	# Events
0.00	10.00	Yes	0.396	53415	0.417	36692	0.401	44541
0.75	0.75	No	0.557	10617	0.569	7338	0.561	9088
0.50	0.75	Yes	0.537	7859	0.566	5442	0.541	6558
1.00	1.25	No	0.627	7324	0.642	5137	0.635	6414
0.75	1.25	Yes	0.612	5143	0.642	3610	0.622	4377
1.25	1.50	No	0.696	4761	0.717	3399	0.705	4215
1.00	1.25	Yes	0.686	3171	0.718	2267	0.695	2750
1.25	1.50	Yes	0.742	2091	0.786	1516	0.755	1827
1.75	1.25	No	0.822	2048	0.844	1507	0.827	1856
1.75	0.75	No	0.835	1670	0.860	1219	0.846	1501
2.00	1.25	No	0.865	1431	0.884	1050	0.871	1291
2.00	1.00	No	0.871	1350	0.890	983	0.881	1203
2.00	1.00	Yes	0.894	661	0.917	492	0.905	565

Table 7: Number of selected gluon tagged events and gluon purity in the sample obtaining by using tracks are compared for different jet algorithms.

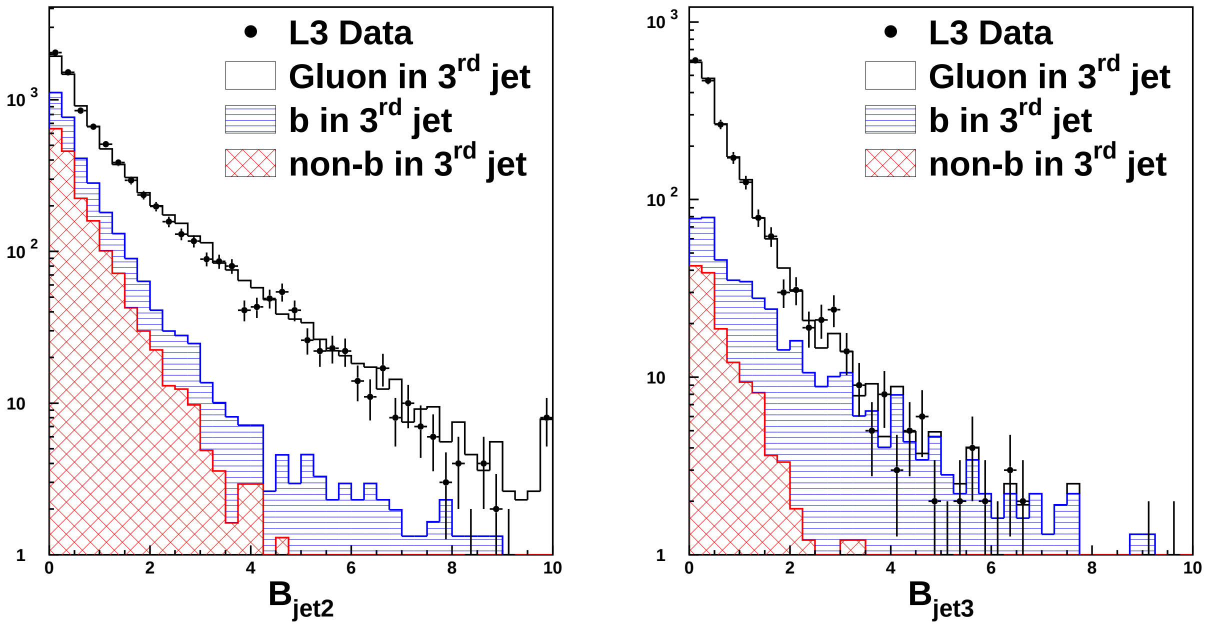

Figure 9: (N-1) cut plots for b-tag for jet 2 and jet 3.

the jet with the lowest b-tag discriminant. This sample of 2048 events corresponds to a purity of 82.2%. The optimum values of the cuts are chosen to provide the highest sensitivity to the differences between colour singlet and colour octet exchange: a balance between gluon purity and statistics of the final event sample.

4 Results

4.1 Measurement of Asymmetry Distributions

The measured distributions at detector level differ from the ones at particle level because of detector effects, limited acceptance and resolution. After subtracting the background obtained from simulations, the measured distributions are corrected for detector effects, acceptance and resolution on a bin-by-bin basis by comparing the detector level results with the particle level results. The level of migration is kept at a negligible level by using a bin size larger than the experimental resolution. We also correct the data for initial and final state photon radiation bin-by-bin using Monte Carlo distributions at particle level with and without radiation.

Figure 10 shows the overall correction factor for asymmetry in bisector angle between quark and gluon jets. One sees the corrections are not too large and the correction factor has a smooth variation over the entire region.

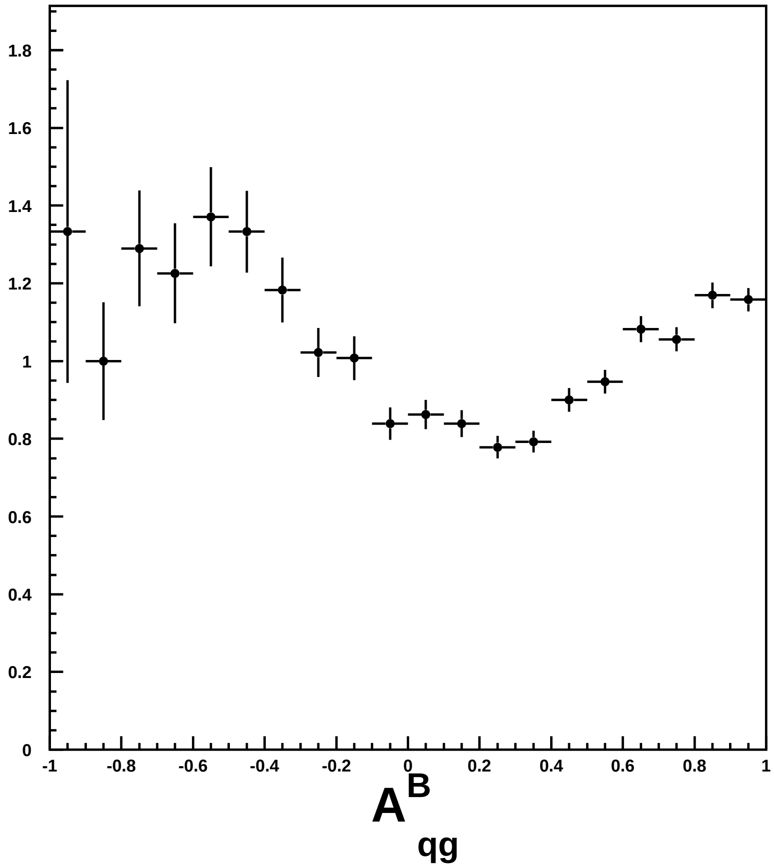

Figure 10: Overall correction factor for asymmetry in bisector angle between quark and gluon jets

4.2 Systematic Uncertainties

The following sources of variations are considered for systematic effects on the distributions:

1. Jet reconstruction: the JADE algorithm is taken as the default with $y_{cut} = 0.05$ and the $k_{\perp}$ algorithm with $y_{cut} = 0.01$, 0.02 are used to estimate the systematic uncertainties.
2. Gluon tagging: We take the sample with $B^{mid}_{jet} = 1.25$ (1.75), $B^{min}_{jet} = 1.50$ (1.25) as the default set for cluster (track) sample and the b-tag cuts for the jets are varied so that the gluon purity changes by 10% from the default value.

For the six asymmetry variables, the variations are averaged over bins (with bin-content > 2% of the sample). We find the overall systematic errors are at the level of 4.4% to 8.4% in the sample with clusters. The systematic errors are summarised in table 8.

	Clusters			Tracks		
Variables	Jet	Gtag	Total	Jet	Gtag	Total
A^N_{12}	5.8	7.9	9.8	6.2	5.6	8.4
A^N_{qg}	2.9	4.6	5.5	4.5	2.6	5.2
A^B_{12}	6.2	4.8	7.9	7.7	4.5	8.9
A^B_{qg}	5.8	3.2	6.6	6.4	2.8	6.9
A^S_{12}	7.2	8.1	10.9	4.9	5.3	7.2
A^S_{qg}	4.1	4.0	5.8	3.7	3.0	4.8

Table 8: Systematic variation (%) for the asymmetry variables for clusters and tracks

The change in definition of the jet core affects the particle flow asymmetry distributions significantly: the effect is 7.2% for clusters. It does not make any appreciable difference in the case of angular asymmetries, which thus have very little bias from fragmentation effects.

4.3 Comparison with Monte Carlo

Figure 11 compares the distributions of particle flow asymmetry from the various Monte Carlo models with the data. The asymmetries are defined with energy clusters and the core of the jet is removed using a 15° cone around the jet axis and the distributions are corrected to particle level. The data are in agreement with the predictions of JETSET and disfavours colour singlet exchange. We also include prediction of RATHSMAN model for a value of 0.1 of the parameter R which determines the probability of string re-interactions and the other fragmentation model parameters are set to L3 defaults for JETSET. The agreement with this model is worse than that with JETSET.

Figure 12 compares the corrected distributions of bisector angle asymmetry between jets 1, 2 and q, g from the different Monte Carlo models with the data. The asymmetries are again defined with energy clusters and the core of the jet is removed using a 15° cone around the jet axis. Here also, the data are in agreement with the predictions of JETSET.

The comparison between data and different model predictions are summarised in table 9 in the form of χ^2. As one can see that colour octet exchange with string fragmentation effect as implemented in JETSET PS Monte Carlo describes best the data. Models with pure colour singlet exchange can be ruled out and even RATHSMAN model is disfavoured.

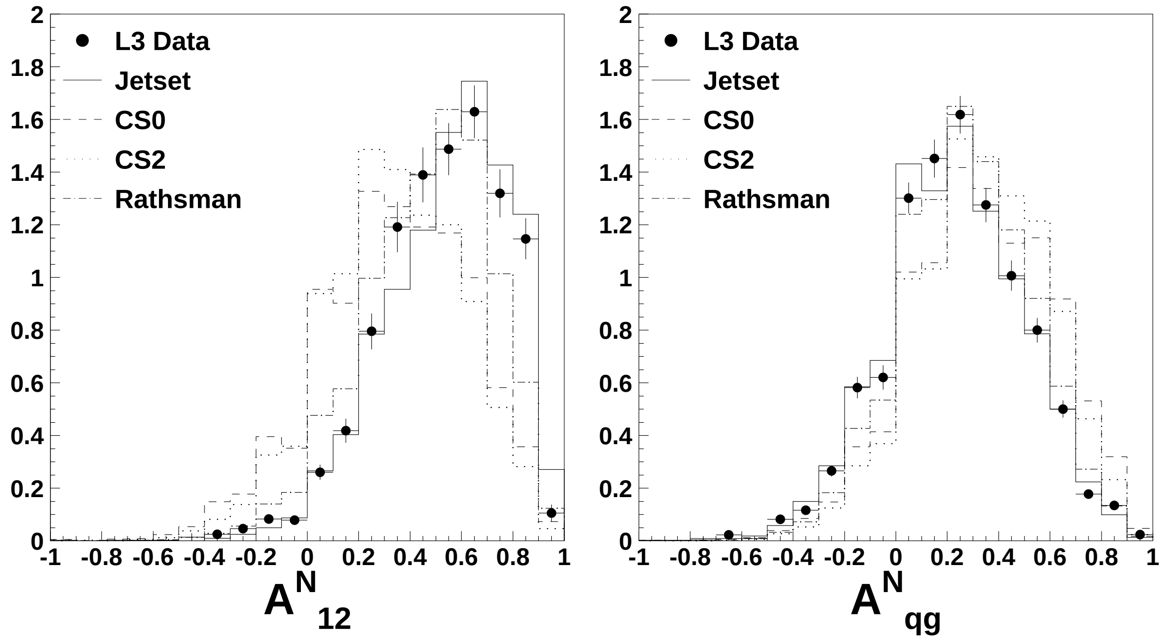

Figure 11: Particle flow asymmetry in the data compared with different Monte Carlo models using clusters. The errors shown are statistical only.

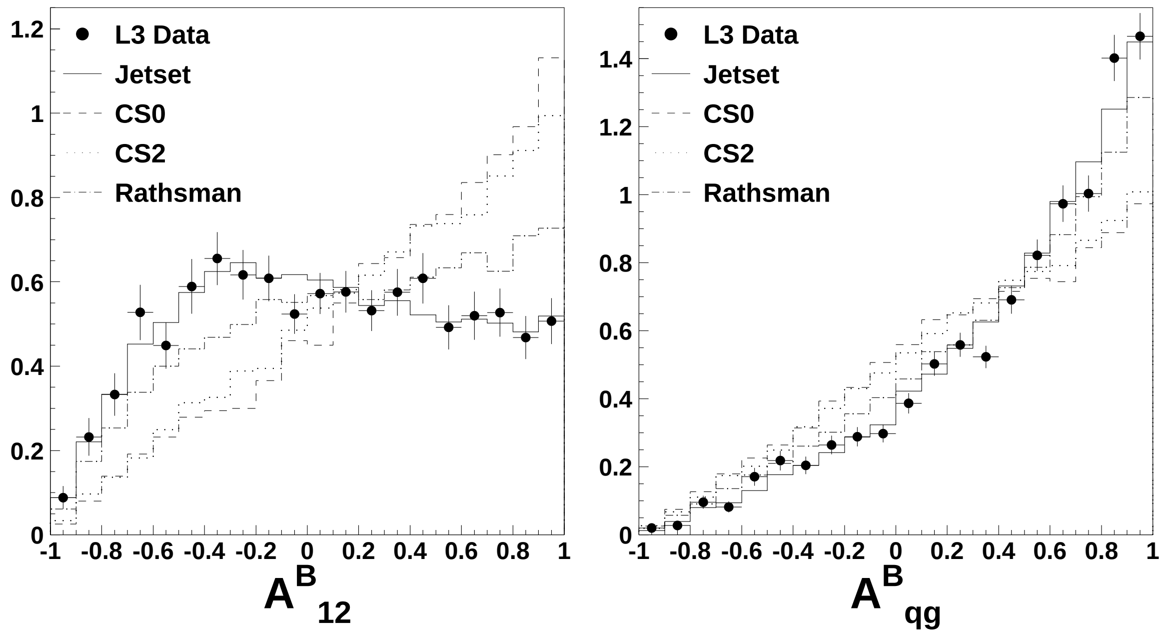

Figure 12: Minimum bisector angle gap asymmetries for clusters. The errors shown are statistical only.

Variable	# Data	χ^2 from clusters for				χ^2 from tracks for		
		JETSET	CS0	CS2	RATHSMAN	JETSET	CS0	CS2
A^N_{12}	14	36.5	1179.9	986.5	103.1	15.2	771.8	421.8
A^N_{qg}	16	30.5	699.0	546.1	98.7	40.4	208.4	188.8
A^B_{12}	20	6.2	345.1	254.0	59.3	14.2	236.2	153.9
A^B_{qg}	19	16.9	251.3	199.6	60.5	13.5	189.2	116.2
A^S_{12}	12	4.7	1074.9	520.2	77.8	14.8	504.2	280.8
A^S_{qg}	13	6.5	324.4	257.2	47.2	9.2	239.2	168.6

Table 9: χ^2 obtained from the comparison of the data distributions to different fragmentation models.

4.4 Fits

All the angular and asymmetry distributions can be fitted to a combination of colour octet exchange (as obtained from JETSET) and a colour singlet contribution. This is done by minimising χ^2 defined as

$$\chi^2(r) = \sum_i \frac{[f^i_{data} - r f^i_{CS} - (1-r) f^i_{\mathrm{JETSET}}]^2}{(\sigma^i_{stat})^2 + (\sigma_{syst} * f^i_{data})^2}$$

where r is the fraction of the colour singlet component and contributions from both statistical and systematic uncertainties are included.

Good fits are obtained to all the asymmetry distributions studied in this analysis. For the most sensitive variable A^S_{12}, the fit gives r = 0.015 $\pm$ 0.030 (χ^2/d.o.f. = 4.5/11). Figure 13 shows results of such fits for CS0 and CS2 models to distributions of asymmetries in the maximum separation angle for gaps between jets 1, 2 and q, g using clusters and corrected to particle level. These fits results from other variables also give fraction of events due to colour singlet exchange consistent with zero. The results of these fits are summarised in table 10.

Variable	Events	CS0		CS2	
		r	χ^2/d.o.f.	r	χ^2/d.o.f.
A^B_{12}	Clusters	0.017$\pm$0.053	6.1/19	0.017$\pm$0.062	6.1/19
	Tracks	0.127$\pm$0.058	9.4/19	0.150$\pm$0.071	9.7/19
A^B_{qg}	Clusters	$-$0.022$\pm$0.067	16.8/18	$-$0.031$\pm$0.076	16.7/18
	Tracks	0.067$\pm$0.070	12.6/18	0.110$\pm$0.087	11.9/18
A^S_{12}	Clusters	0.015$\pm$0.030	4.5/11	0.025$\pm$0.043	4.4/11
	Tracks	0.074$\pm$0.042	11.7/11	0.106$\pm$0.054	11.1/11
A^S_{qg}	Clusters	0.040$\pm$0.054	6.0/12	0.035$\pm$0.061	6.2/12
	Tracks	0.051$\pm$0.062	8.5/10	0.044$\pm$0.076	8.9/10

Table 10: Results from fits to asymmetry distributions with an admixture of colour singlet and colour octet exchanges

So we use the distributions to compute a 95% confidence level upper bound to the fraction of colour singlet exchange. We obtain this upper bound by solving the following equation for

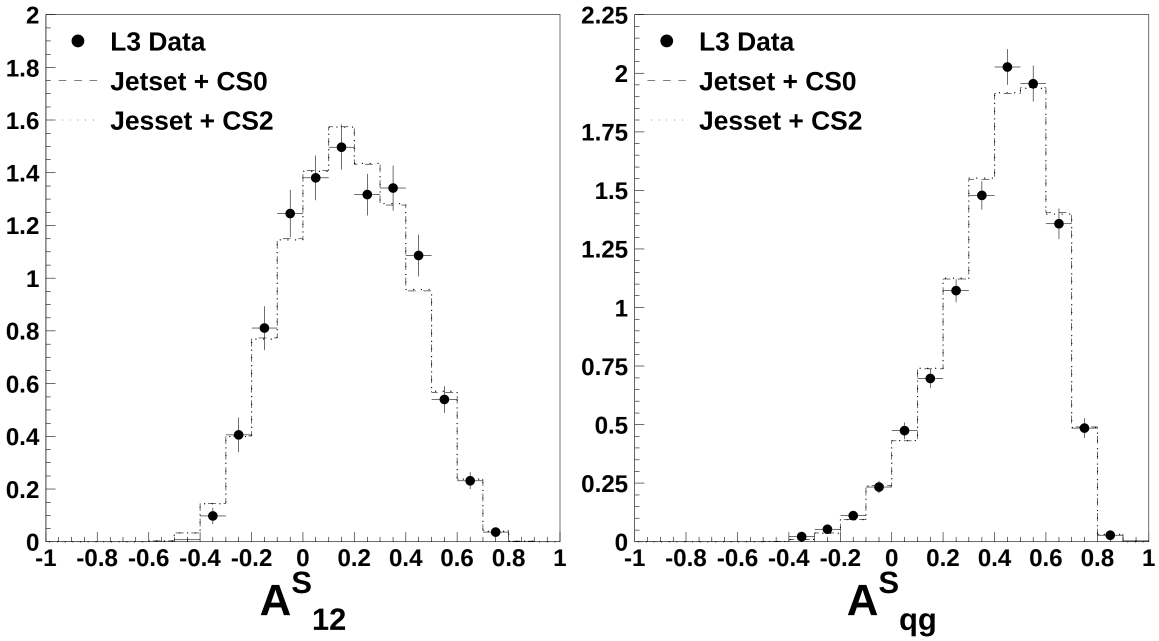

Figure 13: Maximum separation angle gap asymmetries for clusters. The errors shown are statistical only. The dashed and dotted lines are fits to the data using a combination of colour octet and colour singlet contributions using the Cs0 and Cs2 models

each distribution:

$$\int_0^R \exp\left(-\frac{\chi^2}{2}\right) dr \quad = \quad 0.95 \times \int_0^1 \exp\left(-\frac{\chi^2}{2}\right) dr$$

	Bounds for			
	(from clusters)		(from tracks)	
Variables	Cs0	Cs2	Cs0	Cs2
A^B_{12}	11.6 %	13.4 %	22.2 %	26.7 %
A^B_{qg}	11.7 %	13.0 %	18.8 %	25.8 %
A^B_{12} and A^B_{qg}	8.2 %	9.3 %	17.6 %	22.5 %
A^S_{12}	6.9 %	10.2 %	14.3 %	19.6 %
A^S_{qg}	13.5 %	14.5 %	16.1 %	18.0 %
A^S_{12} and A^S_{qg}	6.7 %	9.0 %	12.4 %	15.8 %

Table 11: 95% confidence level upper bound to fraction of colour singlet exchange in Mercedes 3-jet events from hadronic Z decays using various asymmetry distributions

Results from these fits are summarised in table 11. As can be seen from the table, one gets limits around 11% from different asymmetry distributions. The asymmetry variables A^B_{12} and A^B_{qg} are independent and so are A^S_{12} and A^S_{qg}. So one can use a pair of variables to obtain 95% CL upper bounds of the two colour singlet models. From these fits, one gets a most stringent upper bounds of 6.7% (9.0%) for Cs0 (Cs2) model using the pair of variables A^S_{12} and A^S_{qg}. Fits from events using tracks give consistent but somewhat weaker limits.

Fits have been performed to the asymmetry distributions to obtain the best value of the R-parameter in the RATHSMAN model using the distributions obtained at different values of R. Good fits are obtained as shown in figure 14 for bisector angular asymmetries in the two gaps. The results from the fits are summarised in table 12. The values of R obtained from these fits are consistent with zero.

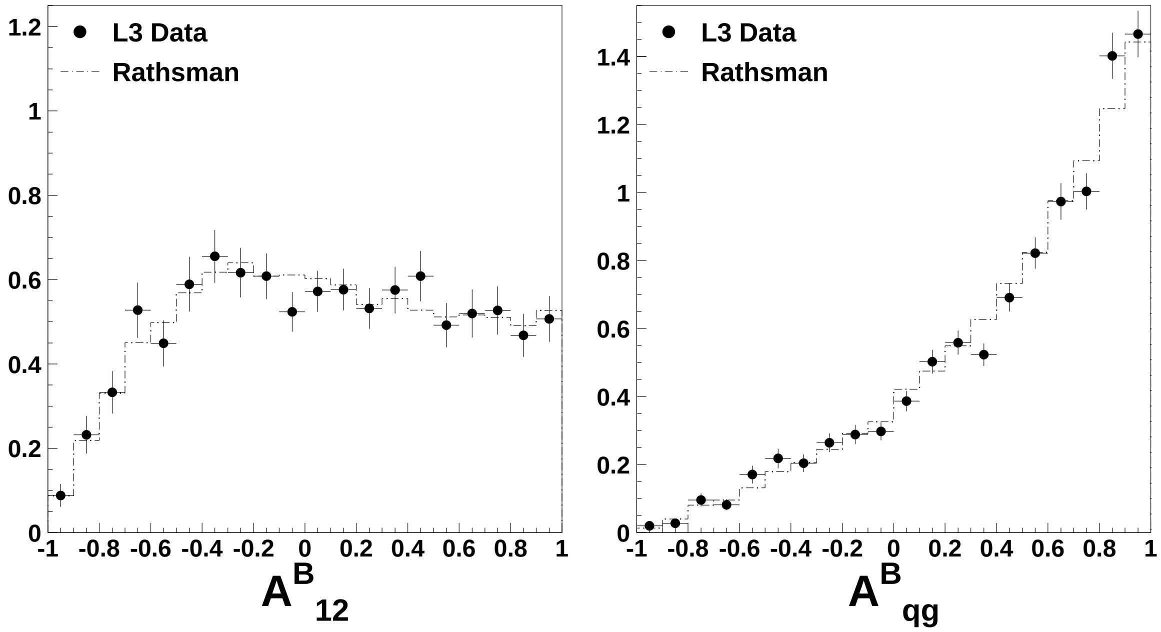

Figure 14: Bisector angle gap asymmetries for clusters. The errors shown are statistical only. The dashed-dotted lines are best fits for RATHSMAN model.

Variable	Events	R	χ^2/d.o.f.
A^B_{12}	Clusters	0.0036±0.0051	5.6/19
	Tracks	0.0031±0.0027	10.4/19
A^B_{qg}	Clusters	−0.0011±0.0056	16.8/18
	Tracks	0.0095±0.0180	13.2/18
A^S_{12}	Clusters	0.0039±0.0062	4.3/11
	Tracks	0.0219±0.0170	12.5/11
A^S_{qg}	Clusters	0.0031±0.0059	6.2/12
	Tracks	−0.0038±0.0152	9.2/10

Table 12: Results from fits to asymmetry distributions for the parameter R in RATHSMAN model

So these distributions can be used to compute a 95% confidence level upper bound on R. A procedure similar to that for the fraction r of colour singlet exchange is followed to obtain this 95% confidence level upper limit. The results are summarised in table 13. As can be seen from the table, one gets limits between 0.012 − 0.017 using single asymmetry distributions. Combining the pair of variables A^B_{12} and A^B_{qg} or A^S_{12} and A^S_{qg}, one can obtain better limits (0.009 or 0.012) for the parameter R.

Variables	Bounds for R	
	(from clusters)	(from tracks)
A_{12}^{B}	0.0141	0.0879
A_{qg}^{B}	0.0124	0.0653
A_{12}^{B} and A_{qg}^{B}	0.0093	0.0598
A_{12}^{S}	0.0165	0.0591
A_{qg}^{S}	0.0160	0.0532
A_{12}^{S} and A_{qg}^{S}	0.0119	0.0405

Table 13: 95% confidence level upper bound to the colour reconnection probability (R) in the RATHSMAN model as obtained from 3-jet events in hadronic Z decays from various asymmetry distributions

5 Summary

We have carried out a search for colour singlet exchange and colour reconnection effect in the asymmetry distribution of angular gaps in the 3-jet sample from hadronic Z decays. We have identified several asymmetry variables which are sensitive to colour singlet exchange and colour reconnection. A particularly powerful discrimination is provided by the bisector angle asymmetry (see figure 12). From a sample of 2 million hadronic Z decays, two independent analyses have been carried out using tracks and calorimetric clusters.

The study reveals that data can be explained by colour octet exchange alone without any significant colour reconnection. We obtain upper limits of colour singlet exchanges from a set of of observables. The two models of colour singlet exchange can contribute at most at the level of 6.7% or 9.0% to the symmetric 3-jet events at the 95% confidence level.

The colour reconnection model is disfavoured by data. A 95% confidence level upper bound of 0.0093 is obtained for colour reconnection probability in the framework of a generalised area law model for hadronic string re-interaction.

References

[1] J. D. Bjorken, Phys. Rev. **D47** (1993) 101.

[2] DØ collaboration, S. Abachi *etal.*, Phys. Rev. Lett. **72** (1994) 2332;
CDF collaboration, F. Abe *etal.*, Phys. Rev. Lett. **74** (1995) 855;
DØ collaboration, S. Abachi *etal.*, Phys. Rev. Lett. **76** (1996) 734;
CDF collaboration, F. Abe *etal.*, Phys. Rev. Lett. **78** (1997) 2698;
CDF collaboration, F. Abe *etal.*, Phys. Rev. Lett. **79** (1997) 2636;
DØ collaboration, B. Abbott *etal.*, Phys. Lett. **B440** (1998) 189;
CDF collaboration, F. Abe *etal.*, Phys. Rev. Lett. **80** (1998) 1156.
CDF collaboration, F. Abe *etal.*, Phys. Rev. Lett. **81** (1998) 5278.
CDF collaboration, T. Affolder *etal.*, Phys. Rev. Lett. **84** (2000) 232.
CDF collaboration, T. Affolder *etal.*, Phys. Rev. Lett. **85** (2000) 4215.

[3] H1 collaboration, T. Ahmed *etal.*, Nucl. Phys. **B429** (1994) 477;
ZEUS collaboration, M. Derrick *etal.*, Phys. Lett. **B332** (1994) 228;
ZEUS collaboration, M. Derrick *etal.*, Phys. Lett. **B369** (1996) 55.

[4] J. Ellis and D. A. Ross, Z. Phys. **C70** (1996) 115.

[5] SLD Collaboration, K. Abe *etal.*, Phys. Rev. Lett. **76** (1996) 4886.

[6] M. M. Block and F. Halzen, 'Survival Probability of Large Rapidity Gaps in $\overline{p}p$, pp, γp and $\gamma\gamma$ Collisions', MADPH-00-1203, hep-ph/0101022.

[7] Z. Kunst *etal.*, Physics at LEP2, edited by G. Altarelli, T. Sjöstrand, F. Zwirner, CERN 96-01 (1996), Vol. 1, 141.

[8] OPAL collaboration, G. Abbiendi *etal.*, Eur. Phys. J. **C11** (1999) 217.

[9] JETSET 7.4 Monte Carlo Program:
T. Sjöstrand, Comp. Phys. Comm. **82** (1994) 74.

[10] L3 Collaboration, B. Adeva *etal.*, Z. Phys. **C55** (1992) 39;
S. Banerjee, M. Sc. Thesis, University of Mumbai (1998);
S. Banerjee *etal.*, L3 Note # 2667 (2001).

[11] M. Unger, L3 note 2322 (1998).

[12] J. Rathsman, Phys. Lett. **B452** (1999) 364.

[13] S. Banerjee *etal.*, L3 note 2715 (2001).

[14] The L3 detector simulation is based on GEANT Version 3.15.
See R. Brun *etal.*, "GEANT 3", CERN DD/EE/84-1 (Revised), September 1987.
The GHEISHA program (H. Fesefeldt, RWTH Aachen Report PITHA 85/02 (1985)) is used to simulate hadronic interactions.

[15] JADE Collaboration, W. Bartel *etal.*, Z. Phys. **C33** (1986) 23;
JADE Collaboration, S. Bethke *etal.*, Phys. Lett. **B213** (1988) 235.

[16] Yu. L. Dokshitzer, Contribution to the Workshop on Jets at LEP and HERA (1990);
N. Brown and W.J. Stirling, Rutherford Preprint RAL-91-049;
S. Catani *etal.*, Phys. Lett. **B269** (1991) 432;
S. Bethke *etal.*, Nucl. Phys. **B370** (1992) 310.

[17] L3 Collaboration, B. Adeva *etal.*, Nucl. Inst. Meth. **A289** (1990) 35;
B. Alpat *etal.*, Nucl. Inst. Meth. **A315** (1992) 197-200;
M. Chemarin *etal.*, Nucl. Inst. Meth. **A349** (1994) 345;
M. Acciarri *etal.*, Nucl. Inst. Meth. **A351** (1994) 300;
M. Acciarri *etal.*, Nucl. Inst. Meth. **A360** (1995) 103-109.

[18] L3 Collaboration, M. Acciarri *etal.*, Phys. Lett. **B411** (1997) 373.